Published in final edited form as:
J Biomed Mater Res A. 2010 May ; 93(2): 505–514. doi:10.1002/jbm.a.32544.

Interplay of Anionic Charge, Poly(ethylene glycol), and Iodinated Tyrosine Incorporation within Tyrosine-derived Polycarbonates: Effects on Vascular Smooth Muscle Cell Adhesion, Proliferation and Motility

Patrick A. Johnson[2,3], **Arnold Luk**[1,3], **Aleksey Demtchouk**[1], **Hiral Patel**[1], **Hak-Joon Sung**[3], **Matthew D. Treiser**[1], **Simon Gordonov**[1], **Larisa Sheihet**[3], **Das Bolikal**[3], **Joachim Kohn**[3], and **Prabhas V. Moghe**[1,2,*]

[1]Department of Biomedical Engineering, New Jersey Center for Biomaterials, Rutgers University, Piscataway, NJ 08854

[2]Department of Chemical and Biochemical Engineering, New Jersey Center for Biomaterials, Rutgers University, Piscataway, NJ 08854

[3]Department of Chemistry and Chemical Biology, New Jersey Center for Biomaterials, Rutgers University, Piscataway, NJ 08854

Abstract

Regulation of smooth muscle cell adhesion, proliferation, and motility on biomaterials is critical to the performance of blood-contacting implants and vascular tissue engineering scaffolds. The goal of this study was to examine the underlying substrate-smooth muscle cell response relations, using a selection of polymers representative of an expansive library of multifunctional, tyrosine-derived polycarbonates. Three chemical components within the polymer structure were selectively varied through copolymerization: 1) the content of iodinated tyrosine to achieve X-ray visibility; 2) the content of poly(ethylene glycol) (PEG) to decrease protein adsorption and cell adhesivity; and 3) the content of desaminotyrosyl-tyrosine (DT) which regulates the rate of polymer degradation. Using quartz crystal microbalance with dissipation, we quantified differential serum protein adsorption behavior due to the chemical components DT, iodinated tyrosine, and PEG: increased PEG content within the polymer structure progressively decreased protein adsorption but the simultaneous presence of both DT and iodinated tyrosine reversed the effects of PEG. The complex interplay of these components was next tested on the adhesion, proliferation, and motility behavior cultured human aortic smooth muscle cells. The incorporation of PEG into the polymer reduced cell attachment, which was reversed in the presence of iodinated tyrosine. Further, we found that as little as 10% DT content was sufficient to negate the PEG effect in polymers containing iodinated tyrosine while in non-iodinated polymers the PEG effect on cell attachment was reversed. Cross-functional analysis of motility and proliferation revealed divergent substrate chemistry related cell response regimes. For instance, within the series of polymers containing both iodinated tyrosine and 10% of DT, increasing PEG levels lowered smooth muscle cell motility without a change in the rate of cell proliferation. In contrast, for non-iodinated tyrosine and 10% of DT, increasing PEG levels increased cell proliferation significantly while reducing cell motility. Clearly, the polycarbonate polymer library offers a sensitive platform to modulate cell adhesion, proliferation, and motility responses, which, in turn, may have implications for controlling vascular remodeling in vivo. Additionally, our data suggests unique biorelevant

*To whom all correspondence should be addressed: Prabhas V. Moghe, Professor, Rutgers University, 599 Taylor Road, Piscataway, NJ 08854, 732-445-4500 X 6315, moghe@rci.rutgers.edu.

properties following the incorporation of iodinated subunits in a polymeric biomaterial as a potential platform for X-ray visible devices.

INTRODUCTION

Regulation of cell adhesion, proliferation, and motility on biomaterials is critical to the performance of biomedical implants and tissue engineering scaffolds. In particular, controlling smooth muscle cell response is crucial for the success of blood contacting devices as well as vascular tissue engineering materials 1. For instance, a major problem in cardiovascular stent applications is restenosis after implantation that is caused by excessive smooth muscle cell proliferation and migration into the intima 2 3. Additionally, in the development of materials for small diameter vascular replacements, hemocompatibility and hyperplasia have remained major obstacles. One approach to regulating cellular responses on biomaterials is to rationally design biodegradable polymers to include chemical properties that provide hemocompatibility and control cell adhesion, proliferation, and motility. Alternatively, it is necessary to promote smooth muscle growth and migration to engineer artificial arterial blood vessels for vascular graft applications as well as for the development of *in vitro* models of vasculature 4. For artificial artery applications, synthetic, biodegradable materials can be used to regulate the structure of smooth muscle cells, fibroblasts, and endothelial cells into functional constructs 5,6. However, in general, studies on new materials for tissue engineering and implant applications are limited to few known polymers with a limited number of conditions evaluated.

Recently, combinatorial polymer synthesis has spurned interest in higher throughput cell and protein evaluation studies for promising biomaterials 7. Cell – material interactions have been evaluated using chemical and property gradient films encompassing a wide range of polymer blend compositions as well as processing conditions 8,9. Studies elucidating the effects of combinatorial polymer composition on embryonic stem cell differentiation have also been undertaken 10. To enable higher throughput evaluation, several groups have developed inkjet inspired spotting techniques to minimize the amount of material required and to enable large arrays of different materials or conditions for the evaluation of cell – material interactions 11⁻14. Challenges for high throughput bioscreening on these biomaterial libraries include developing test platforms for efficient and precise data acquisition as well as the ability to process and analyze the large data sets generated. To this end, we have adopted a customizable grid platform formed by frontal photopolymerization of an optical adhesive that allows microliters of dilute polymeric solutions to be cast in an array format on a single coverslip 15. The platform allows each test site to contact the same experimental solution condition at each step, including the cell suspension solution, which greatly limits experimental variability.

A biodegradable tyrosine-derived poly(DTE carbonate) was modified by co-polymerization with monomers of different chemical functionalities to tune specific physical properties. Specifically, it was modified with poly(ethylene glycol) to improve hemocompatibility; desaminotyrosyl tyrosine (DT) units to increase degradation rates; and iodination of the tyrosine ring to impart X-ray visibility, which is the first such report of iodination of a polymeric biomaterial. This covalent attachment of iodine in the tyrosine ring holds promise as an important platform for the creation of x-ray visible devices. In this sense, a library of polymers with variable composition was established. Despite the rational design of the library to meet with different functionalities, it is not clear how the modifications may singly or in combination affect basic vascular cell interactions with the resultant polymer library.

We selected a subset of the library of poly(desamino tyrosyl tyrosine ethyl ester carbonate)s (poly(DTE carbonate)) to represent a wide range of properties, and examined the attachment, spreading, proliferation, motility responses of human aortic smooth muscle cells in vitro. We report that this subset of the virtual polymer library exhibits some very distinct responsiveness in terms of cellular phenomena. Based on our findings, the polymers can be designed to optimize different cellular properties and thus customize the composition for the ultimately targeted application.

MATERIALS AND METHODS

Polymer synthesis

Tyrosine-derived poly(DTE carbonate) and its copolymers (Figure 1) were synthesized according to published procedures 16,17. The molar fraction of PEG units (Mw = 1000) in the copolymer was varied between 0 – 15 mol% PEG. Poly(D,L-lactide-co-glycolide) (Resomer 506) and poly(L-lactic acid) (Resomer L-206) were purchased from Boehringer Ingelheim (Ridgefield, CT, USA).

Substrate Fabrication

Grid platforms were fabricated as described previously 15. Briefly, a 35 mm glass coverslip was contacted with a well of Norland 82 optical adhesive. A photomask created by printing out a negative of the desired pattern on a simple transparency with a 1200 dpi printer. The sample was then exposed to a collimated long UV wavelength lamp for two minutes at a distance of eighteen inches. Uncured adhesive was washed away with 70% ethanol and then a 50/50 mixture of acetone and 70% ethanol. The grid platform was further cured for one hour, four inches from the UV lamp. Samples were placed in an oven at 60 °C for 24 h to remove residual volatiles.

Six and half microliters of 1% by weight, polymer solutions were solvent cast into the microwells in a solvent rich atmosphere 18. Solutions were prepared by weighing 10 mg of each polymer, diluting each portion with 1 ml of 1.5% methanol and 98.5% methylene chloride solution followed by thorough mixing. Solutions were filtered through 0.45 micron filters to remove large foreign particles. The grid platform was then assembled into a POC-R stage incubator (PeCon GmbH) for cell adhesion, motility and morphology studies.

Protein Adsorption

Quartz crystal microbalance was used to quantify the responsiveness of the subset of polymer library to protein adsorption from complete serum used in cell culture experiments. To this end, 1% w/v polymer solutions in dioxane (Fisher Scientific) were spin-coated onto gold quartz crystals (Q-Sense, QSX 301) at 4000 RPM. Coated crystals were then equilibrated in PBS for up to 18 hours until a stable baseline (drift < −1 Hz/min) was reached. Crystals were mounted in the QCM-D (Q-Sense, E4) and 5% fetal bovine serum was perfused through the system at a flow rate of 24.2 μl/min for 60 minutes. Phosphate buffered saline (PBS) was then perfused through the system for 90 minutes to rinse off non-adherent proteins.

Raw frequency and dissipation data were modeled with supplied software (Q-Sense, Q-Tools) that utilizes the Voigt model 19. Overtones 5 and 7 were used to model the data. The modeling region was chosen from the beginning of the adsorption to the end of the rinse. Layer density was fixed at 1200 kg/m3. Viscosity, shear, and thickness were set within ranges of 0.0005 – 0.01 kg/m-s, 10^5 – 10^{11} Pa, and 10^{-11} – 10^{-7} m, respectively.

Cell Culture

Human Aortic Smooth Muscle Cells were obtained from Cascade Biologics (C-007-5C). Cells were thawed from a frozen cell bank, and maintained in a humidified incubator at 37 °C and 5% CO_2 in MCDB 131 medium from Biosource International (P174-500) supplemented with SingleQuats which contain bovine insulin 0.1 %, gentamiacin sulfate amphotericin-B (GA-1000) 0.1 %, epidermal growth factor, human recombinant (hEGF) 0.1 %, fibroblast growth factor-B, human recombinant (HFGF-B) 0.2 %, and fetal bovine serum (FBS) 5.0 %.

Cell adhesion study

The grid platform with polymer films was assembled into the stage incubator then pre-wet with complete media for 1 h prior to cell seeding. Cells were stained with Cell Tracker Green CMDA (Invitrogen), washed and then seeded at 20,000 cells/cm^2 in complete smooth muscle cell media. After 1 h incubation at 37 °C and 5% CO_2, the cells were washed 3× with sterile PBS. Cells were imaged at 10 × magnification, 488 nm excitation, and 500–535 nm emission. Cell counts were performed with Image-Pro Plus (Media Cybernetics Silver Spring, MD).

Cell Proliferation

Log phase, passage 8 – 9 smooth muscle cells were grown on grids for 48 h and labeled with BrdU for an additional 24 h. Incorporated BrdU was detected by immunocytochemistry using commercially available reagents (BrdU labeling and Detection Kit I; Roche); nuclei were detected by DAPI staining. Cells were imaged using a Nikon TE2000 microscope and growth rate is presented as the fraction of BrdU-labeled nuclei.

Cell Motility

Human Aortic Smooth Muscle Cells were stained with Cell Tracker Green (Invitrogen), and seeded onto the micro well grid in an open cultivation chamber (PeCon) at a density of 20,000 cells/cm^2 and incubated for 6 h. After incubation, the chamber was mounted into a heatable stage insert (Heating Insert P, PeCon). Temperature control was maintained at 37 °C with a temperature control unit (Tempcontrol 37-2 digital, PeCon). Leica confocal software was used to mark *x-y-z* positions and control the motorized stage. Fluorescent images were acquired at 10 × magnification, 488 nm excitation and 500–535 nm emission using a using a Leica TCS SP2 microscope (Leica Microsystems, Inc., Exton, PA). Three images were taken for each polymer film every 10 min for 15 h. Images were then processed using Image-Pro Plus to analyze the paths of the individual migrating cells. For each image, the *x* and *y* location of the cell centroids were recorded throughout each sequence of images. Cell migration rate was quantified by dividing the net displacement of cell paths over the time interval of tracking. The migration rate was averaged over multiple cell paths in each condition (substrate).

RESULTS

Physical Properties

A selection of twelve, tyrosine-derived polycarbonates was evaluated for smooth muscle cell response. Figure 1 depicts the systematic variation of polymer chemistry. Table 1 groups the polymers in four families, each containing varying amounts of PEG (X = 0, 4, and 8%). The four families are: (1) the family of non-iodinated polymers described by the general formula poly(DTE-co-X%PEG_{1000} carbonate); (2) the family of iodinated polymers described by the general formula poly(I_2DTE-co-X%PEG_{1000} carbonate); (3) the family of non-iodinated copolymers of DTE and 10% DT described by poly(DTE-co-10%DT-co-X%PEG_{1000}

carbonate; and (4) the family of iodinated copolymers of DTE and 10% DT described by poly(I_2DTE-*co*-10% I_2DT-co-X%PEG_{1000} carbonate). The glass transition temperatures (T_g) of the dry polymers were determined using Differential Scanning Calorimetry (DSC). The chemical variations had the following effects on the T_g: (1) the incorporation of two iodine atoms into the tyrosine ring substantially increased the T_g of all polymers by about 40 °C; (2) copolymerization with 10% DT moderately increased T_g by 2 –7 °C; and (3) PEG incorporation decreased the T_g by 6–7 °C for every mol % of PEG_{1000}.

Protein Adsorption

The results of the QCM-D studies of serum protein adsorption are shown in Figure 2. A polymer-dependent adsorption of protein was observed where the effects of incorporating PEG_{1000}, DT and iodination of the tyrosine ring are revealed. The thickness of the adsorbed protein layer was similar for the non-PEG containing polymers (DTE, DTE + 10% DT and I2DTE). However, the PEG effects were significantly different for each of the polymer types. For non-iodinated polycarbonates, the addition of PEG_{1000} (8 mol %) resulted in a dramatically decreased adsorption of serum proteins. Polycarbonates containing iodinated tyrosine displayed reduced effect in protein adsorption when compared with the non-iodinated equivalents. The incorporation of 10% DT also reduced the effect of PEG on protein adsorption for the polycarbonates studied.

Cell Adhesion

Cell adhesion was sensitively altered by alterations in the chemical composition of the polymer library. Figure 3a illustrates the decrease in cell attachment caused by an increase in PEG content within the family of poly(DTE-co-X%PEG_{1000} carbonate)s. At X = 8 mol % PEG_{1000}, the number of cells was reduced by 84%. The corresponding family of iodinated polymers, represented by poly(I_2DTE-co-X%PEG_{1000} carbonate) also showed decreasing cell adhesion with increasing PEG_{1000} content, however, the extent of this effect was less pronounced in the presence of iodinated tyrosine (46% reduction at 8 mol % PEG_{1000}). In contrast, the findings for the polymers represented by poly(DTE-co-10% DT-co-X %PEG_{1000} carbonate) were unexpected: These polymers showed a marked increase in the levels of cell adhesion (Figure 3b) with the number of cells increasing more than twofold at 8 mol % PEG_{1000}. The interplay between the presence of DT and PEG in these terpolymers results in a unique increase in cell adhesivity which is not seen in any of the other polymer families studied here. Notably, only minor variations in cell adhesion were observed in the closely-related, iodinated polymers represented by poly(I_2DTE-co-10%I_2DT-co-X %PEG_{1000} carbonate). For an internal control, cell adhesion on both PLGA and PLA was evaluated simultaneously and was found to be 60% of poly(DTE carbonate) or approximately equal to poly(I_2DTE carbonate) (data not shown).

Cell Morphology

As shown in the first and third columns of the panel of images in Figure 4, cultured smooth muscle cells on poly(DTE carbonate) and poly(I_2DTE carbonate) were well spread and extended. However, upon the incorporation of 4 and 8 mol % PEG_{1000}, the cells lose their extended morphology and became largely rounded. In contrast, DT-containing polymers (second and fourth columns) showed extensive cell spreading, even upon the incorporation of up to 8 mol % PEG_{1000}.

Cell Motility and Proliferation Responses and Their Cross-Correlations

To learn about the effects of substrate chemistry on multiple cellular dynamics, the cell proliferation rate was quantified in terms of fraction of cells in the S-phase, and plotted versus cell migration rate.

Trends in cell proliferation behavior can be analyzed independently. For poly(DTE-co-X %PEG_{1000}carbonate), the cell proliferation rate decreased upon incorporation of PEG_{1000} at 4 mol %. However, for poly(DTE-*co*-10%DT-co-X%PEG_{1000} carbonate), the cell proliferation rate increased with increasing PEG_{1000} content. For poly(DTE-*co*-10% DT-*co*-8% PEG1000 carbonate), the proliferation rate was nearly twice that on poly(DTE-*co*-10% DT carbonate) and was higher than for poly(DTE carbonate). For the iodinated polymer series (poly(I_2DTE-*co*-10%DT-co-X%PEG_{1000} carbonate)), the proliferation rate remained unchanged as the PEG_{1000} content was increased.

Cell motility trends are plotted in Figure 5 and can be first tracked in the absence of any PEG_{1000} (compare markers with "0", indicating no PEG in Figure 5). Incorporation of DT in poly(DTE-*co*-10% DT-co-X%PEG_{1000} carbonate), promoted cell motility in relation to that on poly(DTE-co-X%PEG_{1000} carbonate), while the incorporation of iodinated tyrosine lowered cell motility on poly(I_2DTE-co-X%PEG_{1000} carbonate) as well as in poly(I_2DTE-*co*-10%DT-co-X%PEG_{1000} carbonate). These observations indicate that the incorporation of PEG affected cell motility behavior differentially in those polymers that contained both DT and iodinated tyrosine: Modest PEG content in poly(DTE-co-4%PEG_{1000} carbonate) and in the iodinated poly(I_2DTE-co-4%PEG_{1000} carbonate) led to an increase in cell motility, while a decrease in cell motility was observed in all DT containing polymers represented by the formulae poly(DTE-co-10%DT-co-X%PEG_{1000} carbonate) and poly(I_2DTE-co-10%DT-co-X%PEG_{1000} carbonate). The unique polymer that elicited the highest cell motility was poly(DTE-co-4%PEG_{1000} carbonate), while iodinated polymers elicited the lowest values of cell motility. The entire range of cell motility varied over one order of magnitude between the highest and lowest levels seen among the test polymers.

Cross-functional analysis of average cell motility rate versus proliferation reveals the diverse effects of the underlying chemistry on the cellular response (Figure 5). As PEG_{1000} content increased in all iodinated tyrosine-containing copolymers, the proliferation rate remained constant while the average motility rates varied. On the other hand, poly(DTE-*co*-10%DT-co-X%PEG_{1000} carbonate) elicited a strong increase in the levels of proliferation and a steady decrease in cell motility with increases in PEG_{1000} content. Poly(DTE-co-X %PEG_{1000} carbonate) showed the opposite trends, namely a decrease in cell proliferation and an increase in cell motility upon increase in PEG_{1000} content.

DISCUSSION

The development of new polymeric biomaterials has been largely limited to few polymers studied on few conditions at one time. Advances in combinatorial design and production of polymeric materials have necessitated higher throughput evaluation of cell-biomaterial interactions. In this study, we explored the cellular adhesion, motility, and proliferation responses to a 16-member subset of a combinatorially designed library of tyrosine-derived polycarbonates. As candidate substrates for vascular biomaterial applications, this library offers combinatorial multifunctionality in terms of biodegradability, radio-opacity, and bioactivity. In this study, we report that minute changes in the levels of three major components of the library, charge, iodine, and poly(ethylene glycol) can singly or cooperatively shift the cell motility and proliferation behaviors of cultured smooth muscle cells.

Determining the cellular responses to a combinatorial library of polymers requires large numbers of experiments, materials and time. To efficiently evaluate a promising series of biodegradable polymers, we took a systematic approach to explore the trends and interplay of the key changeable chemical components: PEG, iodination, and a free acid containing monomer. To evaluate this range of polymers, we adopted a customizable grid platform

formed by frontal photopolymerization of an optical adhesive that allows microliters of dilute polymeric solutions to be cast in an array format on a single coverslip 15. The platform allows for the application of less than 100 nanograms of polymer and all the polymer test sites see the same cell suspension solution and washing steps limiting experimental variability.

One of the basic ways to characterize the synthesized polymers is through substrate adsorptivity of proteins upon progressive incorporation of PEG. We chose to use fetal bovine serum as a model system to explore protein adsorption. The antifouling properties of PEG_{1000} in biomaterial coatings and as copolymers in synthetic materials has been well documented 20. The presence of PEG in tyrosine derived poly(DTE carbonate) was shown previously to reduce protein adsorption 21 and increase in PEG levels within limits was shown to increase cell motility in keratinocytes 22. The effect of PEG, DT and iodine on protein adsorption was investigated by QCM-D studies. In agreement with previously published studies by Weber et al. 21 the copolymerization of DTE with PEG results in significantly decreased levels of protein adsorption. Further, the incorporation of significantly higher concentrations of PEG has been shown to almost inhibit the adsorption of protein by QCM 23. In our studies, the incorporation of the negatively charged unit DT offset this repulsive effect and even appeared to increase the affinity of the surface to serum proteins compared to DTE. A similar result was reported for the adsorption of fibrinogen on CH_3 and OH terminated SAMs 24. In summary, for non-iodinated polymers, FBS adsorbed readily to DTE, DTE-co-10% DT, and DTE-co-10% DT-co-8% PEG but as expected, not to DTE-co-8% PEG. Interestingly, in I2DTE copolymers and terpolymers, the copolymerization of I2DT and/or PEG appears to make little difference in the surface's ability to adsorb proteins. The results suggest that at these compositions, the bulky iodine atoms may sterically reduce access to DT and PEG segments, and therefore the protein adsorption behavior varies insignificantly. This has been observed in similar QCM studies where iodinated polycarbonates suppress water uptake and the nonfouling capability of PEG is negated (unpublished observations).

To elucidate the direct effect of PEG_{1000} on cell attachment of human aortic smooth muscle cells, we contacted the polymer film array with serum containing media and then seeded 20,000 cells/cm^2. The reduction in the amounts of adsorption of serum containing proteins with increasing PEG_{1000} content was expected to result in fewer cells adhering to the substrates. In fact, we found that at 15 mol % PEG by molar content (data not shown), almost no cells attached. However, upon the incorporation of iodine in the tyrosine ring, the effect of PEG_{1000} was reduced with smaller decreases in the number of adhered cells with progressive incorporation of PEG_{1000}. The presence of the rather large iodine atom alters the physical properties of the polymer by increasing the stiffness of the polymer and increasing the glass transition temperature. This increase in stiffness and reduction of the polymer mobility at 37 °C may inhibit the ability of PEG_{1000} to fully hydrate and achieve its full antifouling capability.

In contrast to PEG effects on cell adhesion, the incorporation of charge promoted cell attachment. France and coworkers showed that low concentrations of carboxylic acids (2.3%) in plasma co-polymers increased attachment of keratinocytes 25. To increase the degradation rate of our polymer, one of the functional endpoints of the library's performance space, we included 10% DT monomer units in the copolymerization. The free carboxylic acid as shown in Figure 1, subjects the polymer to increased hydrolysis rates, thus increasing the rate of degradation (Pesnell and Kohn, unpublished data). With the addition of carboxylic acids we initially found fewer cells attached. However, with increasing amounts of PEG_{1000} up to 8 mol %, the number of cells progressively increased to twice that of the base polymer poly(DTE carbonate). In addition, the high resolution fluorescent images

clearly show that the cells retained the well spread morphology for polymers containing DT and 0 – 8% PEG_{1000}. The large increase in number of cells adhered to the surface required the presence of both 10% DT and PEG_{1000} concentrations over 4 mol %. However, the corresponding protein adsorption studies only reveal a slight increase in the amount of protein adsorbed for the highly adhesive surfaces. Further investigation of the mechanism of action for this adhesive property is needed to reveal whether protein orientation and configuration effects were affected without altering the amount of adsorbed protein. Additionally, water uptake studies may give insight to the cell response to the materials as initial studies suggest that there is an increase in water uptake for the highly cell adhesive DT and PEG_{1000} copolymers. This increase in water may allow more contact points and access to the film by the cells, thus causing an increase in the number of cells adhered to the surface.

An interesting finding is that all polymers investigated elicited more or less comparable levels of smooth muscle cell proliferation rates in the absence of any PEG. The incorporation of PEG, however, altered the spreading and proliferative responses markedly. For example, progressive PEG incorporation promoted cell spreading on the free acid/DT-containing polymers, consistent with the trends in increased proliferation rates. Concomitantly, the rates of cell migration decreased. Thus, PEGylated DT-containing surfaces support increased smooth muscle cell proliferation and limit cell motility. One of the key observations of our study is that 8% PEGylated DT-containing polymers were the most proliferative substrates among the library studied. In contrast, the base polymer (poly(DTE carbonate) without iodine or free acid) showed decreased cell spreading (and decreased cell proliferation) and increased cell motility with increased PEG content, which is consistent with our previous studies that showed that increased PEG on these substrates promotes cell adhesion activity and lowers cell adhesion strength, thereby increasing cell motility. The iodine containing polymers exhibit anomalous behaviors: increased PEG content (within limits) does increase cell motility but by 8% PEG, cells on these polymers are the least proliferative and least motile. The overall combination of iodine and charge, which seem to have divergent PEG-dependency and effects on cell spreading and adhesion, rendered the motility and proliferative responsiveness of the polymers relatively indifferent to PEG content.

In our study, we focused on the adhesion, motility, and proliferation behaviors of smooth muscle cells (SMCs) because of their importance in cardiac vessel repair and remodeling following injury or pathogenesis 27. In particular, hyperplasia is an issue in restenosis that may be mitigated by controlling SMC migration and proliferation as well as limiting SMC activation and matrix remodeling. While this investigation does not focus on the matrix remodeling aspect, we screened the secretion rates of two distinct matrix molecules, collagen and glucosamine, to evaluate whether there was any correlation between cell motility and matrix secretion. Glucosamine is produced from glucose by the hexosamine pathway and is a precursor of Glycosaminoglycan (GAG) biosynthesis. Although elevated glucose levels (hyperglycemia) accelerate atherosclerosis by increasing vascular cell proliferation and growth, recent studies report that glucosamine impairs vascular cell migration, growth, and capillary-like structure formation 28, 29. To the first approximation, we found that cell motility was inversely correlated with matrix secretion; the combined presence of iodine and PEG was found to maximize both collagen and glycoprotein secretion.

In summary, the cross-functional analysis of cell motility versus proliferation revealed the diverse effects of the underlying chemistry on the cellular response. As PEG_{1000} content increases in the copolymers containing iodine and DT, the average cell motility rate decreased without any change in proliferation rate. On the other hand, poly(DTE-*co*-10%DT

carbonate) elicited increasing levels of proliferation with increases in PEG_{1000} content and with an initial drop in average motility. These chemical response signatures can provide guidance in the selection and design of new biomaterials. For example, applications with high adhesivity and proliferation requirements, a scaffold containing 10% DT and PEG_{1000} could be selected; conversely, for vascular materials that limit smooth muscle cell proliferation and restrict intimal hyperplasia, materials with high PEG and low DT content may be appropriate. Such correlations would need to be tested further using in vivo correlates. A parallel approach currently underway in our laboratory entails the elucidation via surrogate modeling methods of how combination of complex substrate components can concertedly control protein adsorption and cell dynamic behavior.

Acknowledgments

We gratefully acknowledge primary support under the auspices of NIH Grant P41 EB001046 for the biomedical technology resource RESBIO (P. Moghe, J. Kohn). P. Johnson was supported by a NIH T32 fellowship from the NIH T32 HL-07942 Postdoctoral Training Program on Tissue Engineering and Biomaterials Science. Additional support was received from Equipment Lease Fund, Strategic Resource Opportunity Award, Academic Excellence Fund at Rutgers University, and the New Jersey Center for Biomaterials.

REFERENCES

1. Miller DC, Thapa A, Haberstroh KM, Webster TJ. Endothelial and vascular smooth muscle cell function on poly(lactic-co-glycolic acid) with nano-structured surface features. Biomaterials. 2004; 25:53–61. [PubMed: 14580908]
2. Mitra AK, Agrawal DK. In stent restenosis: bane of the stent era. Journal of Clinical Pathology. 2006; 59(3):232–239. [PubMed: 16505271]
3. Kohn J, Zeltinger J. Degradable, drug-eluting stents: a new frontier for the treatment of coronary artery disease. Expert Rev Med Devices. 2005; 2(6):667–671. [PubMed: 16293093]
4. Edelman ER. Vascular tissue engineering: designer arteries. Circ. Res. 1999; 85:1115–1117. [PubMed: 10590236]
5. Davis ME, Hsieh PCH, Grodzinsky AJ, Lee RT. Custom design of the cardiac microenvironment with biomaterials. Circ. Res. 2005; 97:8–15. [PubMed: 16002755]
6. Smith JA. Will Tissue Engineering become the 21st Century's Answer to Cardiovascular Disease? Heart, Lung and Circulation. 2002; 11:135–137.
7. Weber N, Bolikal D, Bourke SL, Kohn J. Small changes in the polymer structure influence the adsorption behavior of fibrinogen on polymer surfaces: validation of a new rapid screening technique. J Biomed Mater Res A. 2004; 68(3):496–503. [PubMed: 14762929]
8. Meredith JC, Sormana JL, Keselowsky BG, Garcia AJ, Tona A, Karim A, Amis EJ. Combinatorial characterization of cell interactions with polymer surfaces. J Biomed Mater Res A. 2003; 66(3): 483–490. [PubMed: 12918030]
9. Simon CG Jr. Eidelman N, Kennedy SB, Sehgal A, Khatri CA, Washburn NR. Combinatorial screening of cell proliferation on poly(L-lactic acid)/poly(D,L-lactic acid) blends. Biomaterials. 2005; 26(34):6906–6915. [PubMed: 15939467]
10. Anderson DG, Levenberg S, Langer R. Nanoliter-scale synthesis of arrayed biomaterials and application to human embryonic stem cells. Nat Biotechnol. 2004; 22(7):863–866. [PubMed: 15195101]
11. Roth EA, Xu T, Das M, Gregory C, Hickman JJ, Boland T. Inkjet printing for high-throughput cell patterning. Biomaterials. 2004; 25:3707–3715. [PubMed: 15020146]
12. Tourniaire G, Collins J, Campbell S, Mizomoto H, Ogawa S, Thaburet J-F, Bradley M. Polymer microarrays for cellular adhesion. Chem. Commun. 2006; 20:2118–2120.
13. Ilkhanizadeh S, Teixeira AI, Hermanson O. Inkjet printing of macromolecules on hydrogels to steer neural stem cell differentiation. Biomaterials. 2007; 28:3936–3943. [PubMed: 17576007]
14. Zhang R, Liberski A, Khan F, Diaz-Mochon JJ, Bradley M. Inkjet fabrication of hydrogel microarrays using in situ nanolitre-scale polymerisation. Chem. Commun. 2008; 11:1317–1319.

15. Cabral JT, Hudson SD, Harrison C, Douglas JF. Frontal photopolymerization for microfluidic applications. Langmuir. 2004; 20(23):10020–10029. [PubMed: 15518489]
16. Yu C, Kohn J. Tyrosine-PEG-derived poly(ether carbonate)s as new biomaterials. Part I: synthesis and evaluation. Biomaterials. 1999; 20(3):253–264. [PubMed: 10030602]
17. Kohn, J.; Bolikal, D.; Pendharkar, SM. Rutgers, The State University of New Jersey, assignee. Radio-opaque polymeric biomaterials. United States Patent. # 6852308. 2005.
18. Kim G, Libera M. Morphological development in solvent-cast polystyrene-polybutadiene-polystyrene (SBS) triblock copolymer thin films. Macromolecules. 1998; 31(8):2569–2577.
19. Voinova MV, Rodahl M, Jonson M, Kasemo B. Viscoelastic acoustic response of layered polymer films at fluid-solid interfaces: Continuum mechanics approach. Physica Scripta. 1999; 59:391–396.
20. Tziampazis E, Kohn J, Moghe PV. PEG-variant biomaterials as selectively adhesive protein templates: model surfaces for controlled cell adhesion and migration. Biomaterials. 2000; 21(5): 511–520. [PubMed: 10674816]
21. Weber N, Wendel HP, Kohn J. Formation of viscoelastic protein layers on polymeric surf aces relevant to platelet adhesion. Journal of Biomedical Materials Research Part A. 2005; 72A(4):420–427. [PubMed: 15678483]
22. Sharma RI, Kohn J, Moghe PV. Poly(ethylene glycol) enhances cell motility on protein-based poly(ethylene glycol)-polycarbonate substrates: a mechanism for cell-guided ligand remodeling. J Biomed Mater Res A. 2004; 69(1):114–123. [PubMed: 14999758]
23. Weber N, Pesnell A, Bolikal D, Zeltinger J, Kohn J. Viscoelastic Properties of Fibrinogen Adsorbed to the Surface of Biomaterials Used in Blood-Contacting Medical Devices. Langmuir. 2007; 13:3298. [PubMed: 17291015]
24. Roach P, Farrar D, Perry CC. Interpretation of protein adsorption: Surface-induced conformational changes. Journal of the American Chemical Society. 2005; 127(22):8168–8173. [PubMed: 15926845]
25. France RM, Short RD, Dawson RA, MacNeil S. Attachment of human keratinocytes to plasma co-polymers of acrylic acid octa-1,7-diene and allyl amine octa-1,7-diene. Journal of Materials Chemistry. 1998; 8(1):37–42.
26. Macario DK, Entersz I, Bolikal D, Kohn J, Nackman GB. Iodine inhibits anti-adhesive effect of PEG: implications for tissue engineering. J. Biomed. Mater. Res. B. Appl. Biomater. 2008; 86:237–244. [PubMed: 18161808]
27. Grewe PH, Deneke T, Machraoui A, Barmeyer J, Muller KM. Acute and chronic tissue response to coronary stent implantation: Pathologic findings in human specimen. J. Am. Coll. Cardiol. 2000; 35:157–163. [PubMed: 10636274]
28. Duan W, Paka L, Pillarisetti S. Distinct effects of glucose and glucosamine on vascular endothelial and smooth muscle cells: evidence for a protective role for glucosamine in atherosclerosis. Cardiovascular Diabetology. 2005; 4:16. [PubMed: 16207378]
29. Luo B, Soesanto Y, Mclain DA. Protein Modification by O-Linked GlcNAc Reduces Angiogenesis by Inhibiting Akt Activity in Endothelial Cells. Arteriosclerosis, Thrombosis, and Vascular Biology. 2008; 28:651.
30. Ghosh D, Krokhin O, Antonovici M, Ens W, Standing KG, Beavis RC, Wilkins JA. Lectin affinity as an approach to the proteomic analysis of membrane glycoproteins. J Proteome Res. 2004; 3(4): 841–850. [PubMed: 15359739]
31. Young NM, Brisson JR, Kelly J, Watson DC, Tessier L, Lanthier PH, Jarrell HC, Cadotte N, St Michael F, Aberg E, Szymanski CM. Structure of the N-linked glycan present on multiple glycoproteins in the Gram-negative bacterium, Campylobacter jejuni. J Biol Chem. 2002; 277(45): 42530–42539. [PubMed: 12186869]

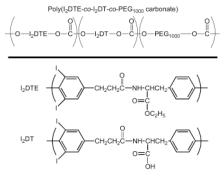

Figure 1.
General chemical structures of tyrosine-derived polymers and possible variation in their I_2DTE, I_2DT, and poly(ethylene glycol) (PEG) content. ‘DTE’ stands for desaminotyrosyl-tyrosine ethyl ester. The tyrosine ring is iodinated. ‘DT’ stands for desaminotyrosyl-tyrosine. The molar fraction of PEG (Mw 1000 g/mol) units in the copolymer was varied between 0–15 mol % PEG and the molecular weight of the PEG blocks was 1000. In I_2DTE and I_2DT, the desaminotyrosyl ring is iodinated.

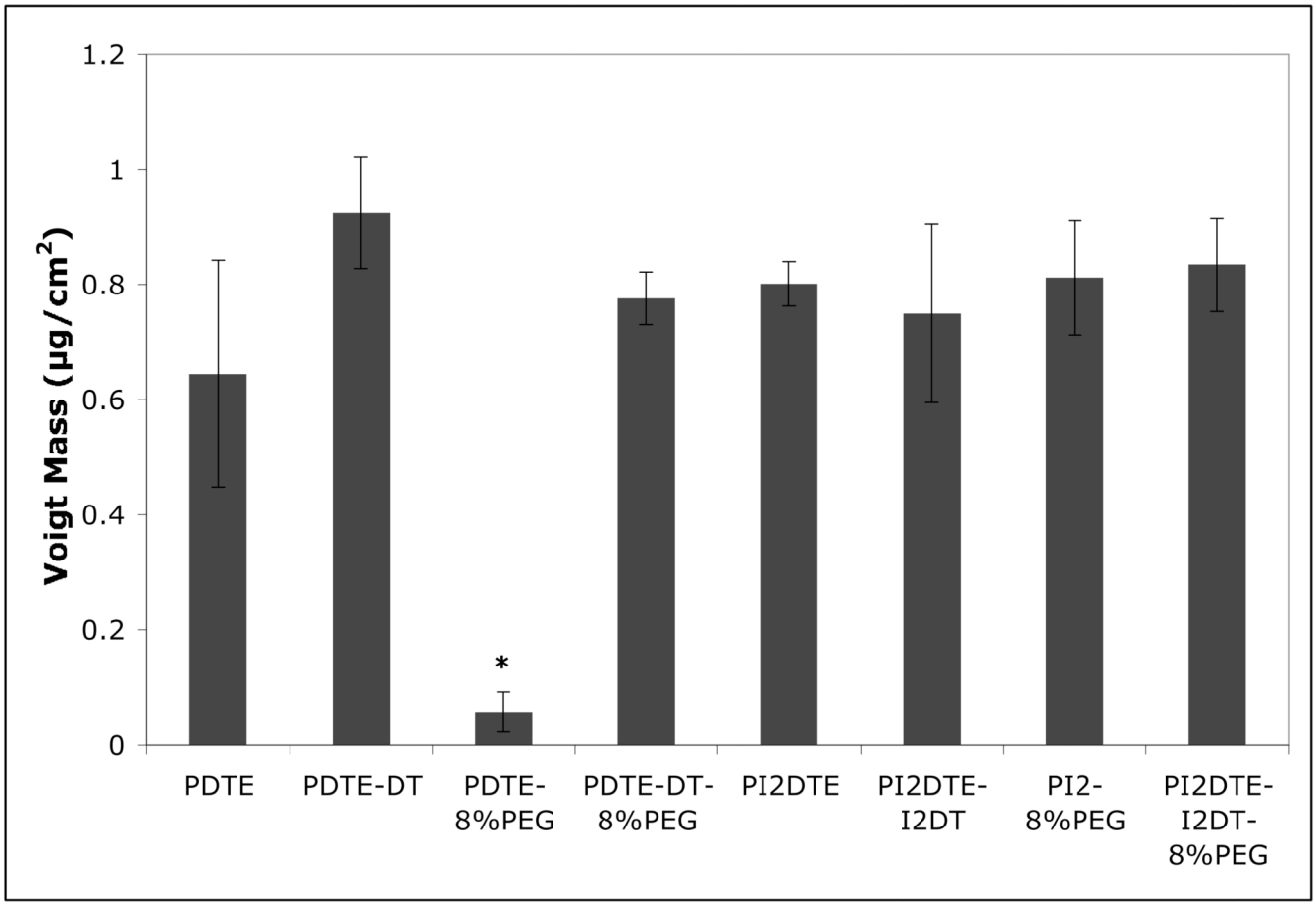

Figure 2.

Protein adsorption behaviors onto substrates coated with tyrosine-derived polymers. * $P<0.05$ vs. the other test groups in the graph. The adsorption of proteins from 5% fetal bovine serum (FBS) was examined on eight test polycarbonate surfaces by perfusion of FBS through the system at a flow rate of 24.2 µl/min for 60 minutes. Phosphate buffered saline (PBS) was then perfused through the system for 90 minutes to rinse off non-adherent proteins. The Voigt model19 was used to calculate the adsorbed protein mass in µg/cm^2: 8% PEG copolymerized with DTE shows a significant decrease in adsorbed protein, but exhibits no protein repulsion when copolymerized with I_2DTE or when polymerized in a terpolymer with 10% DT and DTE.

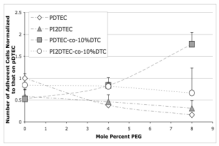

Figure 3.

Polymer chemistry effects on smooth muscle cell attachment. Films were formed by solvent casting, pre-wet with complete medium for 1 hr, and contacted with 20,000 cells/cm^2 for 1 h. Cells were stained with Cell Tracker Green (Invitrogen), imaged at 10× magnification and counted. Cell number was normalized to the number of cells attached to the homopolymer, poly(DTE carbonate) (pDTEC). Note: pDTEC was significantly different than pDTE-4%PEGc and pDTE-8%PEGc ($p < 0.05$); pDTE-DT-8%PEGc was significantly different than pDTE-DTc and pDTE-DT-4%PEGc ($p < 0.075$). No other differences were statistically observed within any grouping of polymers.

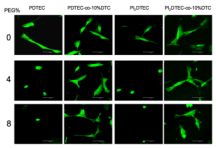

Figure 4.
Polymer chemistry effects on cell morphology. Cells were stained with Cell Tracker Green CMDA, washed and then seeded at 20,000 cells/cm^2 on solvent-cast polymer films pre-wet with media for 1 hour, washed after one hour of incubation, and visualized under confocal microscope.

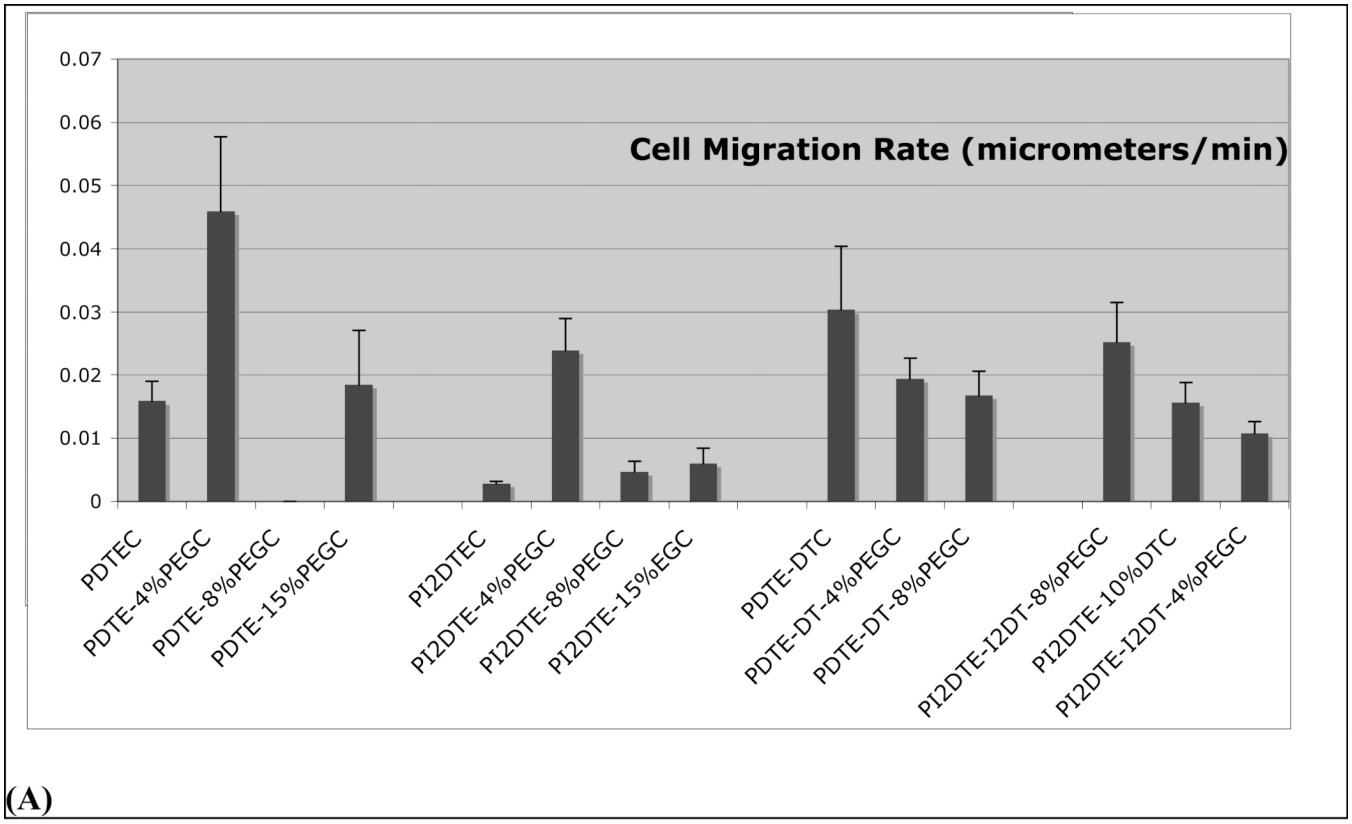

(A)

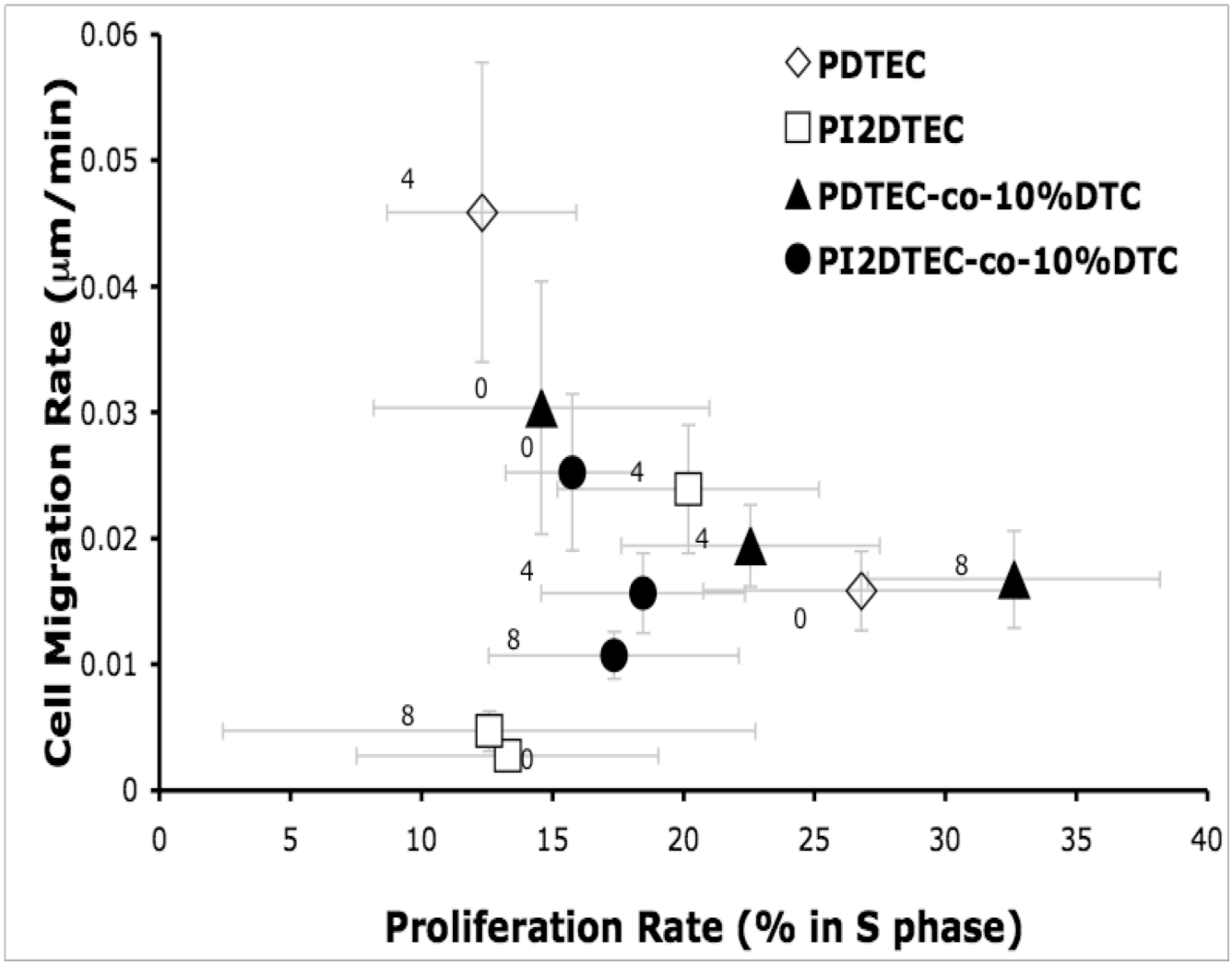

(B)

Figure 5.

Role of combinatorial variation in composition of a subset of tyrosine-derived polymer library on cell migration rate and cell proliferation rate.

(A) Cell migration rates were computed in terms of net distance traveled per unit time. (B) Cross-relations between cell proliferation and migration responsiveness were examined corresponding to changes in substrate chemistry. Unmodified poly(DTE carbonate) polycarbonates promote cell proliferation and support basal cell motility. The incorporation of iodinated tyrosine (poly(I_2DTE carbonate)) lowers both proliferation and motility, while incorporation of charge (with iodinated tyrosine: poly(I_2DTE-*co*-10% DT carbonate), or without iodinated tyrosine: poly(DTE-*co*-10%DT carbonate)) promotes motility while reducing proliferation. Distinct trends in cell motility and proliferation behaviors were observed as a result of progressive incorporation of poly(ethylene glycol) (PEG), indicated by 0,4, and 8 mole % PEG on the figure. i) For poly(I_2DTE-*co*-10% DT carbonate) series of polymers, as PEG_{1000} is added the migration rate decreases but the proliferation rate remains unchanged. ii) For the series, poly(DTE-*co*-10%DT carbonate)), PEG_{1000} increases the rate of proliferation with an initial drop in motility. iii) PEG_{1000} decrease the proliferation rate

for poly(DTE carbonate), but increases the motility. iv) For poly(I_2DTE carbonate) the motility peaks at 4% PEG_{1000} with no significant change in proliferation rate.

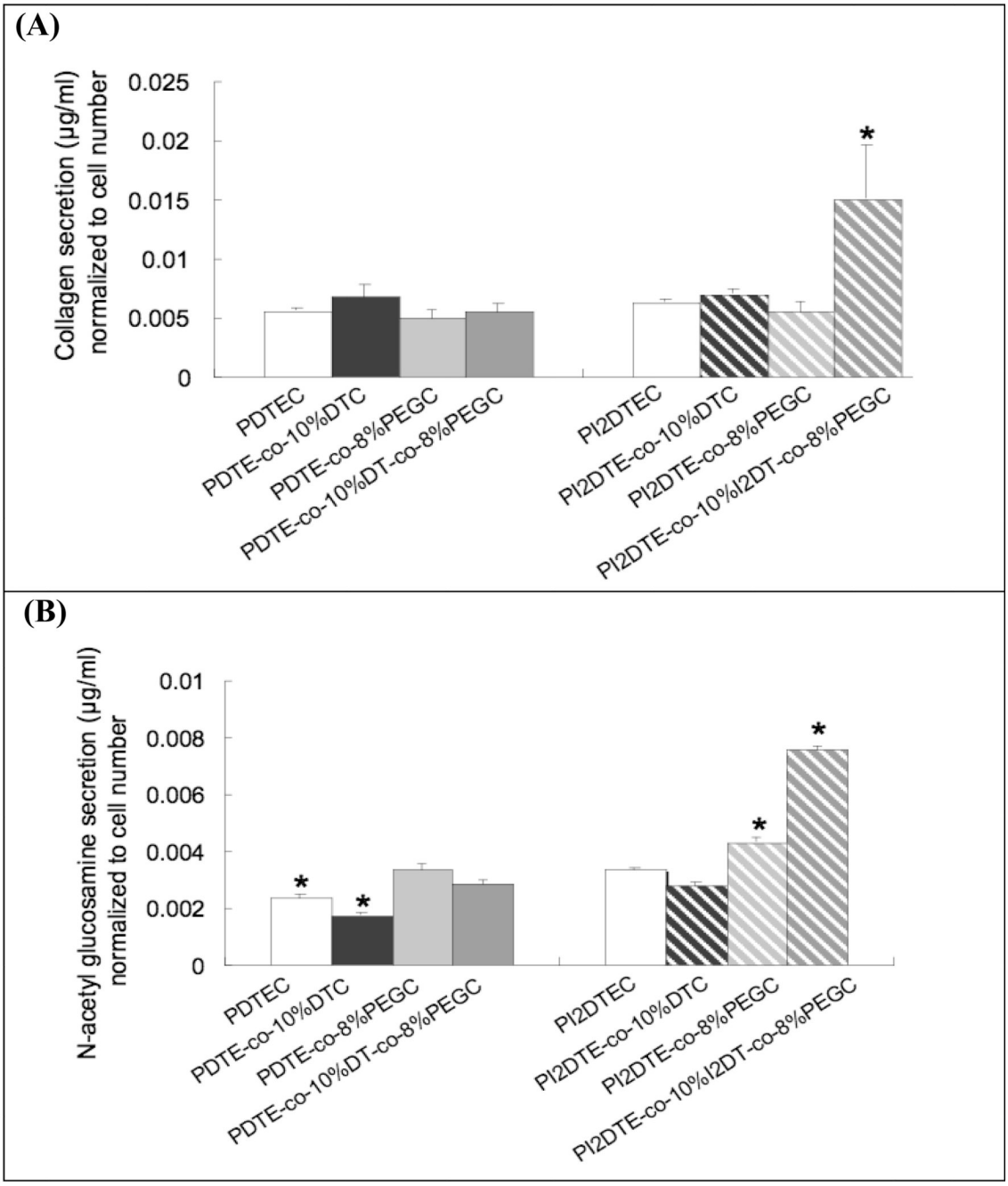

Figure 6.

Smooth muscle cell matrix secretion on the subset of tyrosine-derived polycarbonates was quantified after 3 days in culture in terms of (A) collagen secretion; and (B) N-acetyl glucosamine secretion. * $P<0.05$ vs. the other test groups in the graph. Glycoproteins in extracellular matrix proteins were isolated with the glycoprotein isolation kit (Pierce, Rockford, IL) 30, 31. Briefly, the extracellular matrix proteins and cells were harvested using collagenase type 1 and trypsin. The amount of collagen was measured via a colorimetric assay based on Picro-Sirus Red staining (Direct red 80, Sigma, MO). N-acetyl glucosamine content was measured by passing extract (200 µg per each condition) through an affinity column immobilized with wheat germ agglutinin lectin-agarose, washing, elution,

and quantification with BCA protein assay kit (Pierce). For the series, poly(I2DTE-co-10%I2DT-co-8%PEG1k carbonate) promotes collagen secretion significantly, while the other test groups support the basal level of collagen secretion. The following trends were observed with glycoprotein secretion: The incorporation of iodine and/or PEG in polymers promoted glycoprotein secretion, while the incorporation of charge in the polymers lowered glycoprotein production. A marked increase in glycoprotein production was observed on poly(I_2DTE-co-10%I_2DT-co8% PEG_{1k}carbonate).

Table 1

Representative subset of a library of tyrosine-derived polymers evaluated for smooth muscle cell adhesion, motility, and proliferation. See Figure 1 for chemical structural details on the polymers.

Polymer description	Mn	Mw	Tg
poly(100%DTE carbonate)	127KDa	179KDa	98 °C
poly(96%DTE-co-4%PEG1K carbonate)	128KDa	174KDa	67 °C
poly(92%DTE-co-8%PEG1Kcarbonate)	176KDa	263KDa	44 °C
poly(90%DTE-co-10%DT carbonate)	241KDa (201 kDa)	316KDa (266 KDa)	101 °C
poly(86%DTE-co-10%DT-co-4%PEG1K carbonate)	136KDa	185KDa	71 °C
poly(82%DTE-co-10%DT-co-8%PEG1K carbonate)	120KDa	171KDa	46 °C
poly(100%I_2DTE carbonate)	182KDa (257 kDa)	294KDa (440 kDa)	141 °C
poly(100%I_2DTE carbonate)	257KDa	440KDa	141 °C
poly(96%I_2DTE-co-4%PEG1K carbonate)	139KDa	232KDa	108 °C
poly(92%I_2DTE-co-8%PEG1K carbonate)	316KDa	326KDa	81 °C
poly(85%I_2DTE-co-15%PEG1K carbonate)	178KDa	260KDa	43 °C
poly(90% I_2DTE-co-10% I_2DT carbonate)	241KDa	209KDa	141 °C
poly(86% I_2DTE-co-10% I_2DT-co-4%PEG1K carbonate)	137KDa	196KDa	111 °C
poly(82% I_2DTE-co-10% I_2DT-co-8%PEG1K carbonate)	134KDa	191KDa	85 °C